5. Conclusions

Distributions in TB-climatology of the temperature, ozone and the squared Brunt Väisälä frequency were constructed as a function of the altitude and time for every year and station. Seasonal mean profiles also in TB-climatology were calculated for these quantities. A secondary ozone maximum, located just above the tropopause at high latitude, for the studied time interval was observed every year from late spring and until to summer with varying amplitude. Stronger inversion was observed at higher latitude and during winter the inversion is bigger. It was shown that this second maximum is related to the TIL, with the lower boundary at the tropopause and as its upper limit the lower inflexion point of the static stability profile above the static jump at the tropopause.

A second ozone maximum, located just above the tropopause at high latitude is found every year in late spring and summer with varying amplitude. It is shown that the second ozone maximum is related to the temperature inversion layer. We demonstrate that the troposphere inversion layer at high latitudes is very stable, restricting the vertical transport. The inversion layer ozone is dynamically controlled by horizontal advection. Above the tropospheric inversion layer, the ozone is controlled rather more chemically and is destroyed catalytically. As a result of both processes, a second ozone maximum is built up.

Acknowledgements

R. Werner was supported by the EU 6th FP within the ALOMAR eARI Project. The authors gratefully acknowledge the NOAA Air Resources Laboratory (ARL) for the provision of the HYSPLIT transport and dispersion model. We also thank to the ECMWF team for making available the ERA-40 data.

References

Bell, S. W., Geller, M. A. Tropopause inversion layer: Seasonal and latitudinal variations and representation in standard radiosonde data and global models. J. Geophys. Res. 113, D05109, 2008.

Birner, T., Dörnbrack, A. and Schumann, U., "How sharp is the tropopause at midlatitudes", Geophys. Res. Lett. 29(14), 1700, 2002.

Birner, T. Fine-scale structure of the extratropical tropopause region. J. Geophys. Res., 111, D04104, 2006.

Fahey, D. W., Gao, R.S., Del Negro, L.A., et al. Ozone destruction and production rates between spring and autumn in the Arctic stratosphere. Geophys. Res. Lett. 27, 2605-2608, 2000.

Grewe, V. The origin of ozone. Atmos. Chem. Phys. 6, 1495-1511. 2006,

Holton, J. R. Haynes, P. H., McIntyre M. E., et al. Stratosphere-troposphere exchange. Reviews of. Geophys. 33, 403-439, 1995.

Hwang, S.-H., Kim, J. K., Cho, G.-R. Observation of secondary ozone peaks near the tropopause over the Korean Peninsula associated with stratosphere-troposphere exchange. J. Geophys. Res. 112, D13305, 2007.

Kivi, R., Kyrö, E., Turunen, T., et al. Ozone sondes observations in the Arctic during 1989-2003: Ozone variability and trends in the lower stratosphere and free troposphere. J. Geophys. Res. 112, D08306, 2007.

Krizan , P., Lastovicka, J. Trends in positive and negative laminae in the Northern Hemisphere. J. Geophy. Res. 110, D10107, 2005.

Lemoina, R. Secondary ozone maxima in ozone profiles. Atmos. Chem. Phys. 4, 1085-1096, 2004.

Manney, G. L., Michelsen, H. A., Irion, F. W. et al. Lamination and polar vortex development in fall from ATMOS long-lived trace gases observed during November 1994. J. Geophys. Res. 105, 29,023–29,038, 2000.

Mantis, H.T., Repapis C.C, Zerefos, C.S. The summer maximum in total ozone over northwest Europe. Pure Appl. Geophys. 119, 213-230, 1981.

Melo, S. M., Blatherwick, R., Davies, J., et al., Summertime stratospheric processes at northern mid-latitudes: comparison between MANTRA balloon measurements and the Canadian Middle Atmosphere Model. Atmos. Chem. Phys. 8, 2057-2071, 2008.

Narayana Rao, T., Arvelius, J., Kirkwood, S., et al. Climatology of ozone in the troposphere and lower stratosphere over the European Arctic. Adv. Space Res. 34, 754-758, 2004.

Osterman, G. B., Salawitch, R. J., Sen, B., et al. Balloon-borne measurements of stratospheric radicals and their precursors: Implications for the production and loss of ozone. Geophys. Res. Lett. 24, 1107-1110, 1997.

Pierce, R. B., Grant W. B. Seasonal evolution of Rossby and gravity wave induced laminae in ozone data obtained at Wallops Island, Virginia. Geophys. Res. Lett. 25, 1859– 1862, 1998.

Reid, S. J., et al. A study of ozone laminae using diabatic trajectories, contour advection and photochemical trajectory model simulations. J. Atmos. Chem. 30, 187– 207, 1998.

Rex, M., Salawitch, R.J., von der Gathen, P., et al. Arctic ozone loss and climate change. Geophys. Res. Lett. 2004, 31, L04116, 2004.

Tomikawa, Y., Sato, K., Kita, K., et al. Formation of an ozone laminae due to differential advection revealed by intensive observations. J. Geophys. Res. 107, 4092, 2002.

Solomon, S., "Stratospheric Ozone Depletion: A Review of Concepts and History", Rev. Geophysics, 37, 275-316, 1999.

von der Gathen, P., Rex, M., Harris, N. R. P., et al. Observational evidence for chemical ozone depletion over the Arctic in winter, 1991-92. Nature, 3752, 131-134, 1995.

Figure Captures:

Fig.1. The reconstructed ozone distributions obtained from the ozone lidar measurements at ALOMAR and by the Sodankylä ozone sonde profiles during the overlapping measurement period from December 2000 until November 2001 are very similar because both stations studied approximately the same ozone volume.

Fig.2. The yearly temperature distribution and the seasonal and yearly means in TB-climatology for the observations at Ny Ålesund from December 1999 until November 2000 outlines very clearly the sharp temperature gradient change at the tropopause with a subsequent inversion layer above (a). The temperature inversion generates a sharp jump of the temperature gradient at the tropopause (b).

Fig.3. Static stability distribution derived from the observations at Ny Ålesund from December 1999 until November 2000 in TB-climatology. The temperature gradient jump generates high static stability at the tropopause, which restricts the vertical dynamics, particularly in summer.

Fig.4. a) Ozone number density distribution observed at Sodankylä from December 1999 until November 2000. b) The same as in a) but for the deviations from the yearly mean for every altitude.

Fig.5. Observed Sodankylä temperature profiles and ozone number density profiles during a low tropopause event (05.07.2000) and a high tropopause one (19.07.2000).

Fig.6. Ozone mixing ratio at the 200 hPa pressure level, based on the calculations of ERA-40 daily data. Backward traectories calculated by the HYSPLIT model are drawn on the ozone mixing ratio map. The 4 trajectories for 19.07.2000 (upper panel) and 05.07.2000 (bottom panel) are calculated for 48 hours with a 12 hours step.

Fig.7. Mean seasonal profiles for the temperature (left panels), squared static stability (middle panels) and ozone number density (right panels) for the observations at Sondankylä (at top) and for Ny Ålesund (at bottom) for the time period from 1994 until 2004. The altitudes are related to the tropopause in TB-climatology. The horizontal lines represent approximately the bottom and the upper limit of the temperature inversion layer. The second ozone maximum, obtained in the seasonal means, is situated in the temperature inversion layer just above the tropopause and is related to the horizontal dynamics as a result of the large static stability of the inversion layer.

Figure1
Click here to download high resolution image

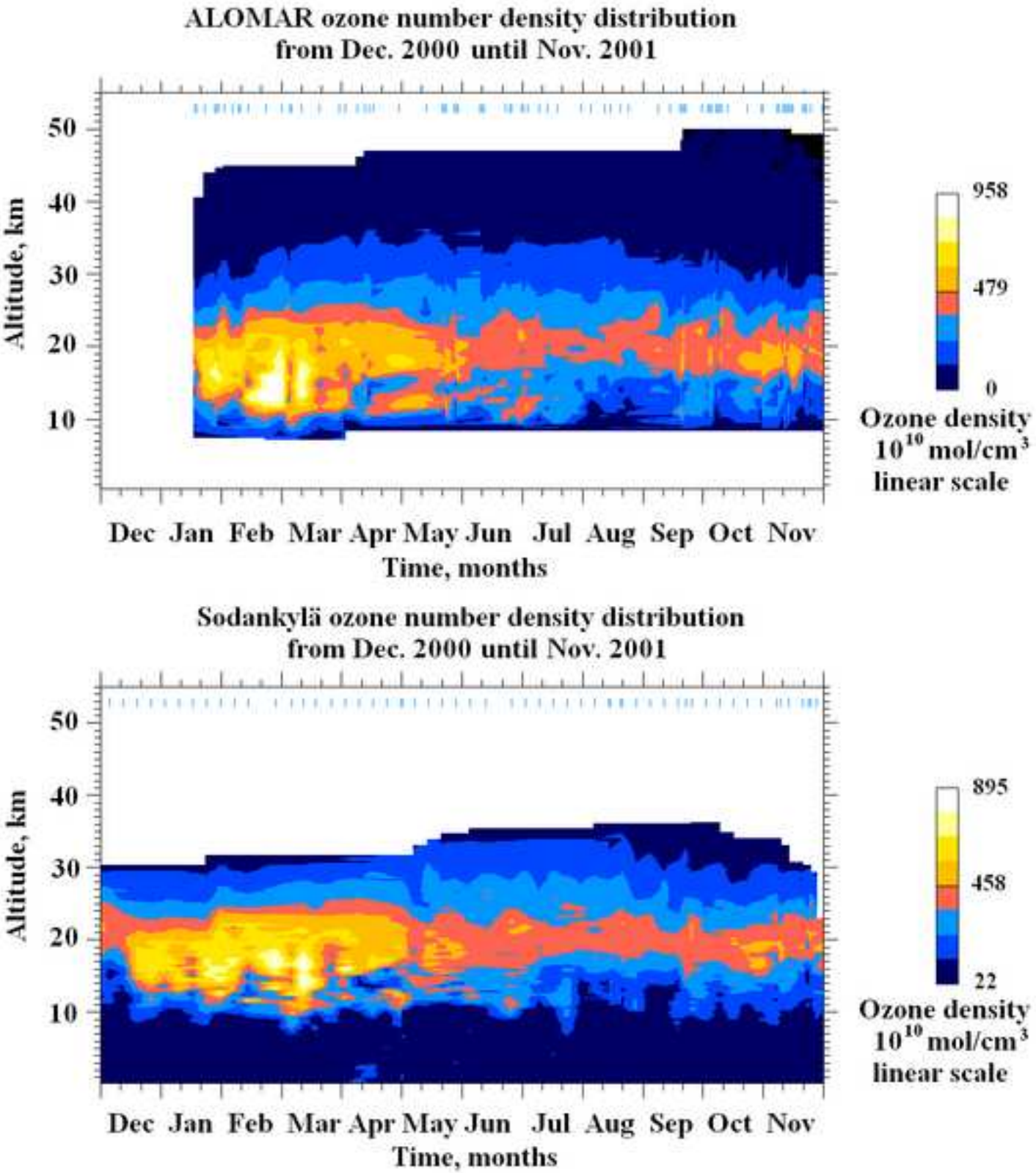

DOI til publisert versjon / DOI to published version: 10.1016/j.asr.2010.09.029

Figure2

Click here to download high resolution image

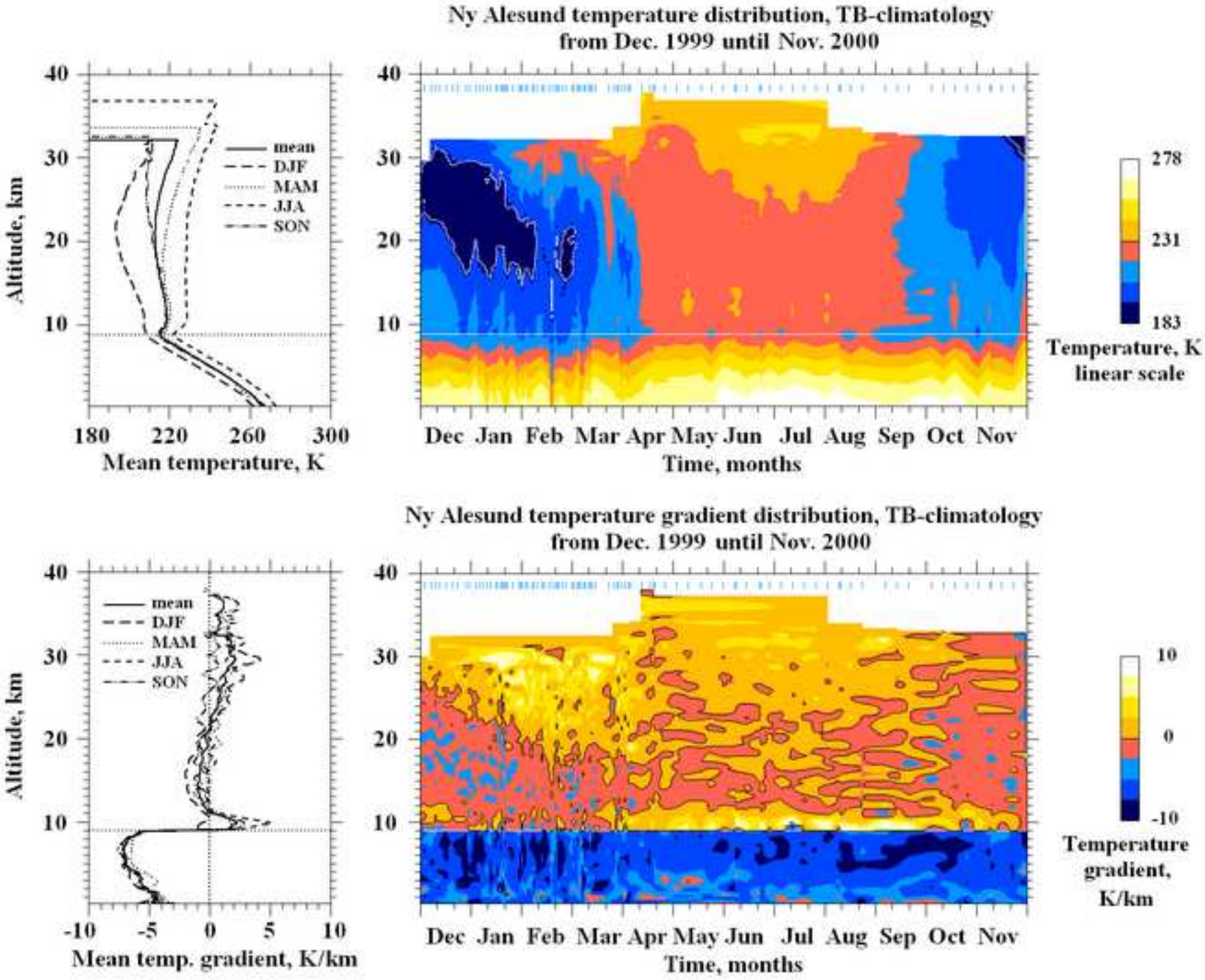

Dette er en postprint-versjon / This is a postprint version.
DOI til publisert versjon / DOI to published version: 10.1016/j.asr.2010.09.029

Figure3
Click here to download high resolution image

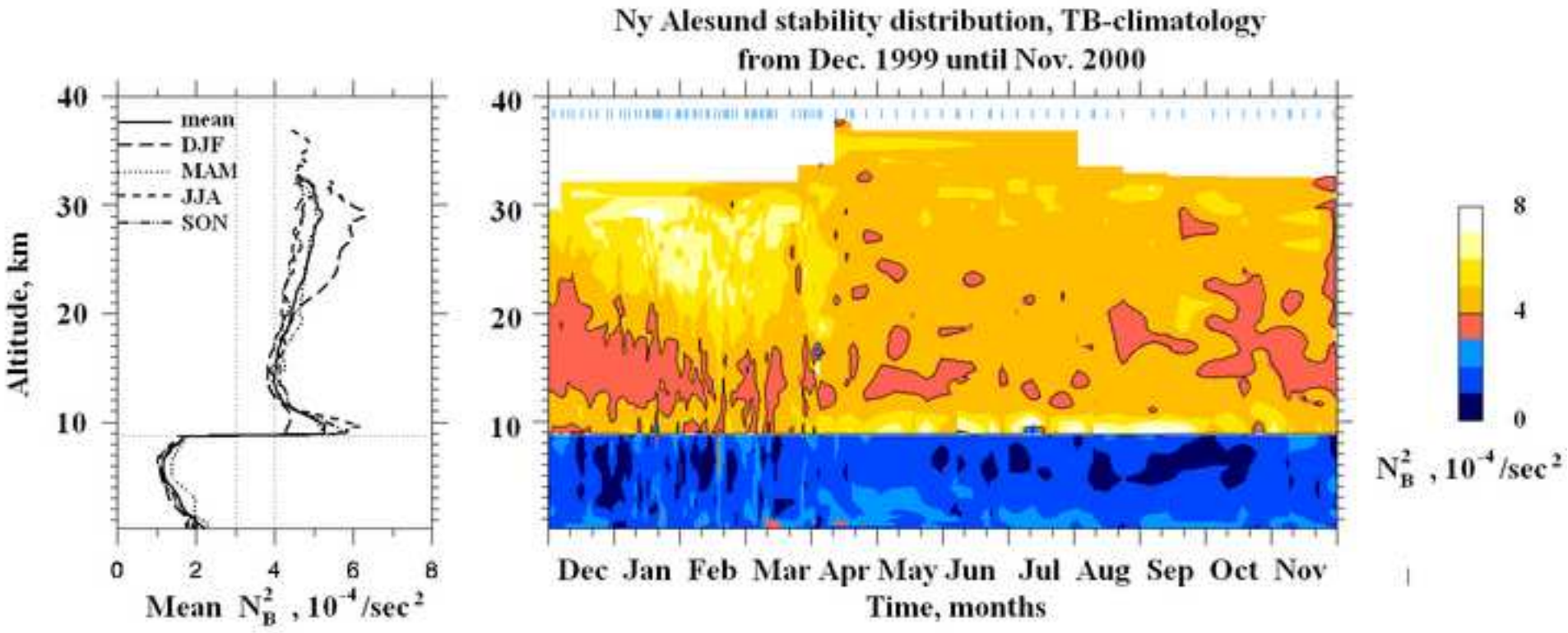

DOI til publisert versjon / DOI to published version: 10.1016/j.asr.2010.09.029

Figure4

Click here to download high resolution image

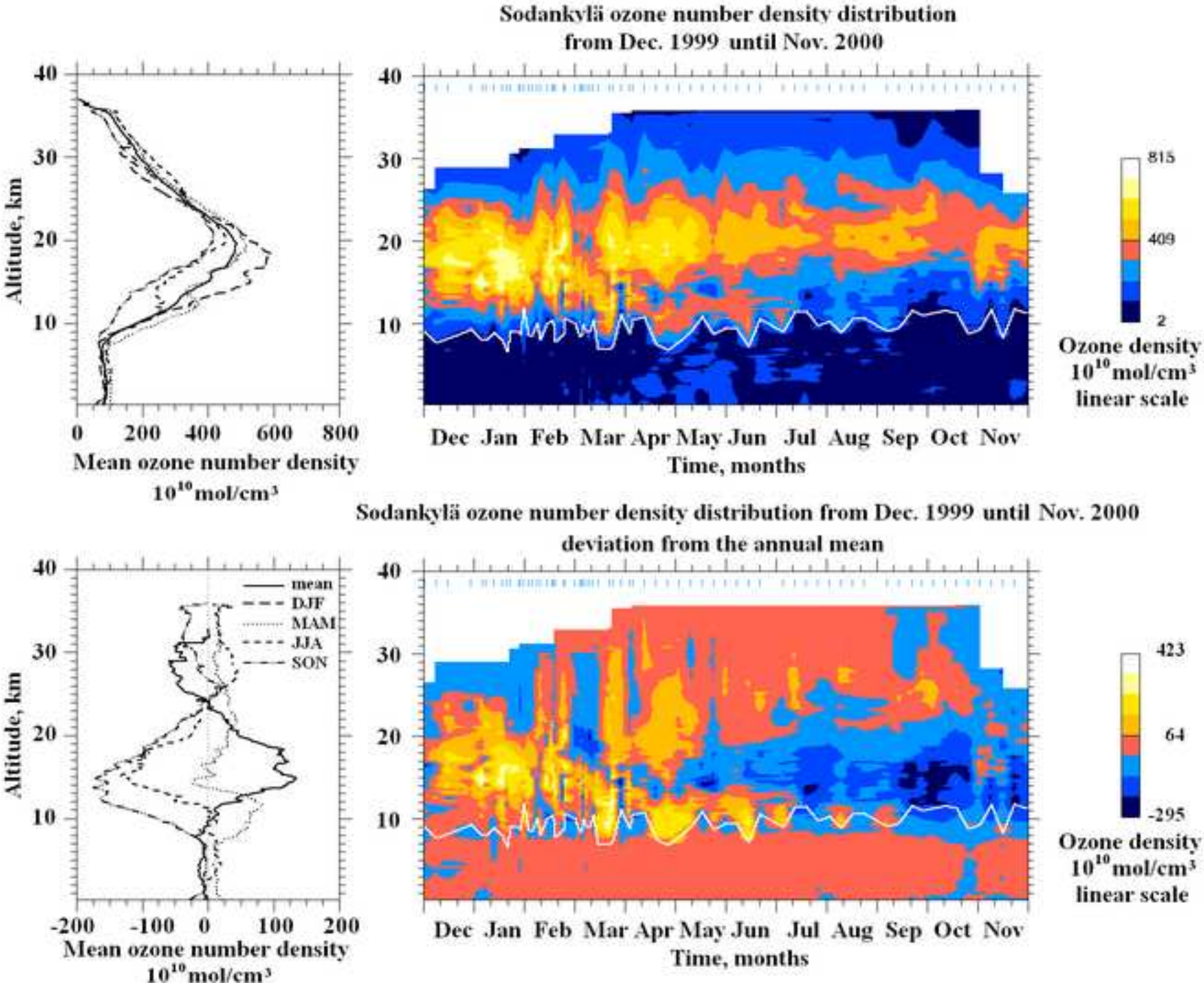

Dette er en postprint-versjon / This is a postprint version.
DOI til publisert versjon / DOI to published version: 10.1016/j.asr.2010.09.029

Figure5
Click here to download high resolution image

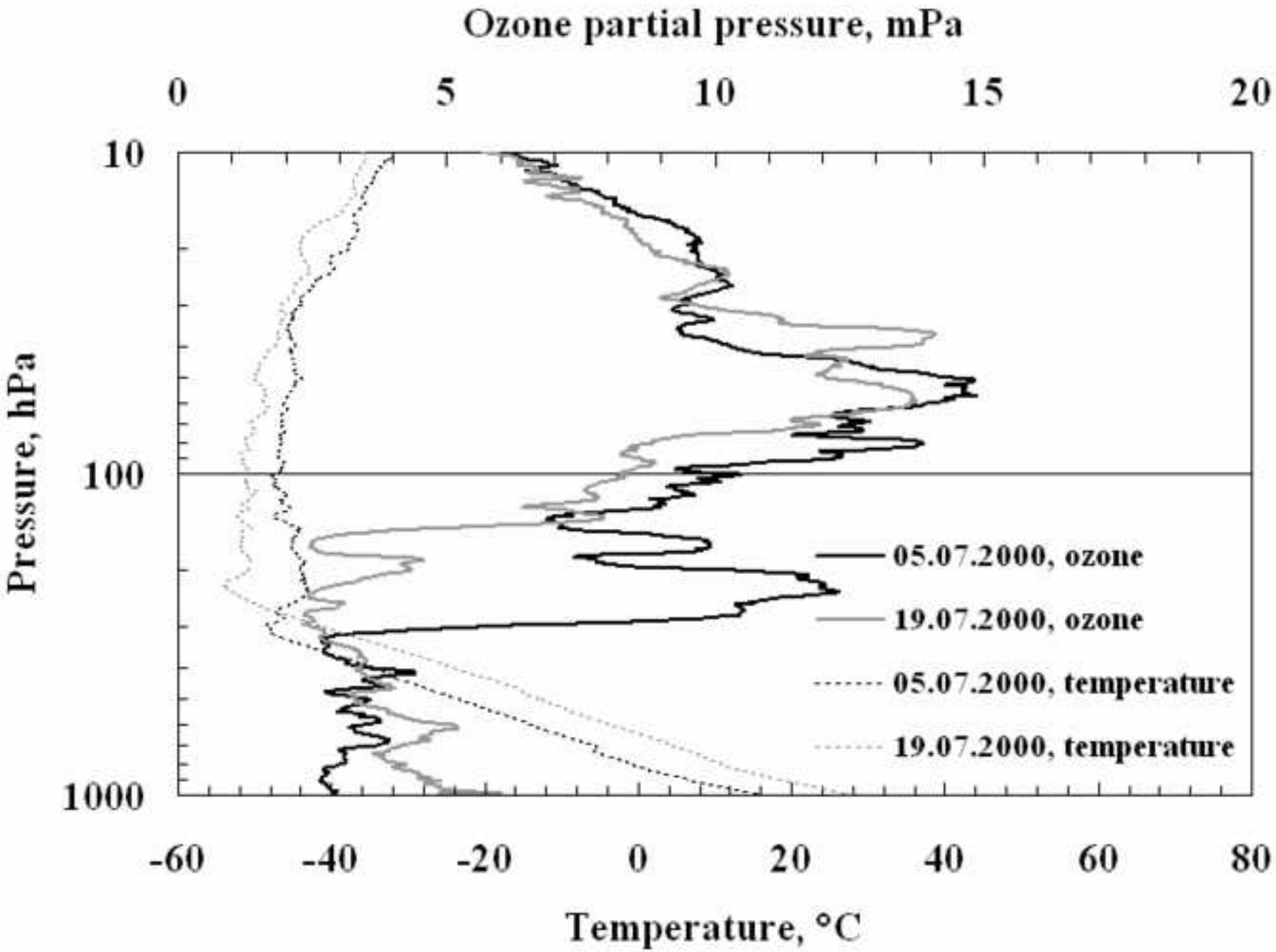

Dette er en postprint-versjon / This is a postprint version.
DOI til publisert versjon / DOI to published version: 10.1016/j.asr.2010.09.029

Figure6
Click here to download high resolution image

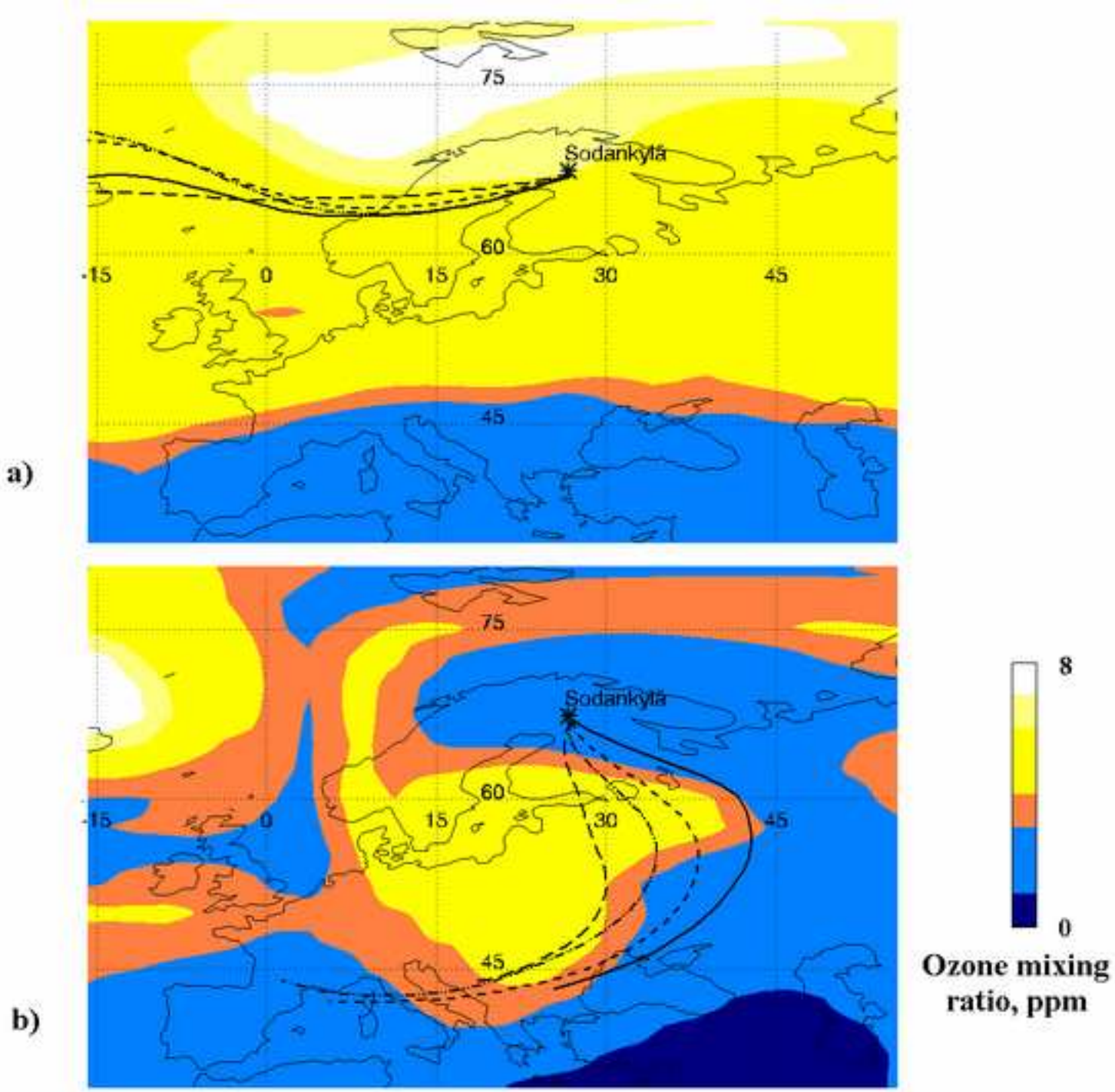

Dette er en postprint-versjon / This is a postprint version.
DOI til publisert versjon / DOI to published version: 10.1016/j.asr.2010.09.029

Figure7

Click here to download high resolution image

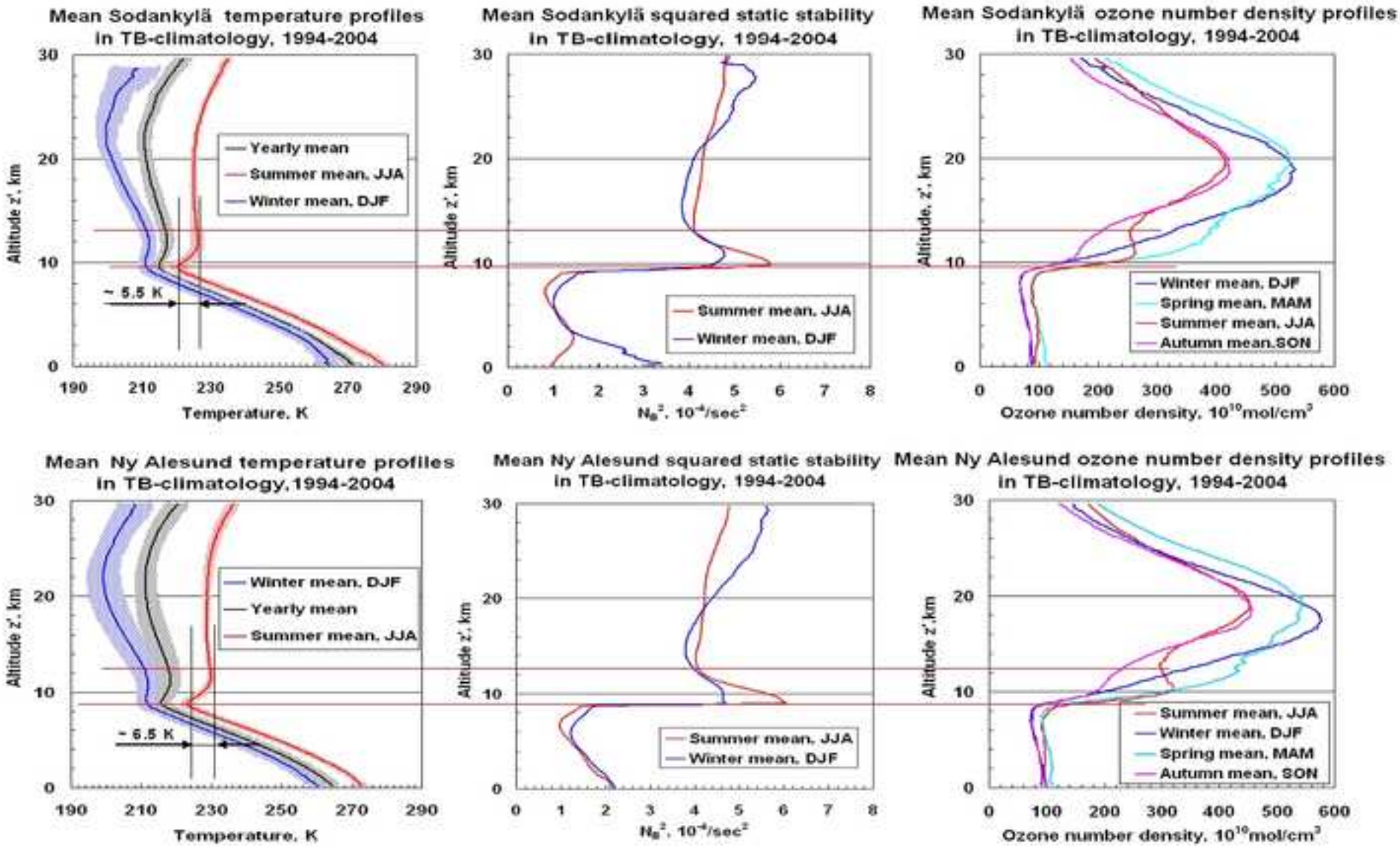

DOI til publisert versjon / DOI to published version: 10.1016/j.asr.2010.09.029